

Supplementary Files

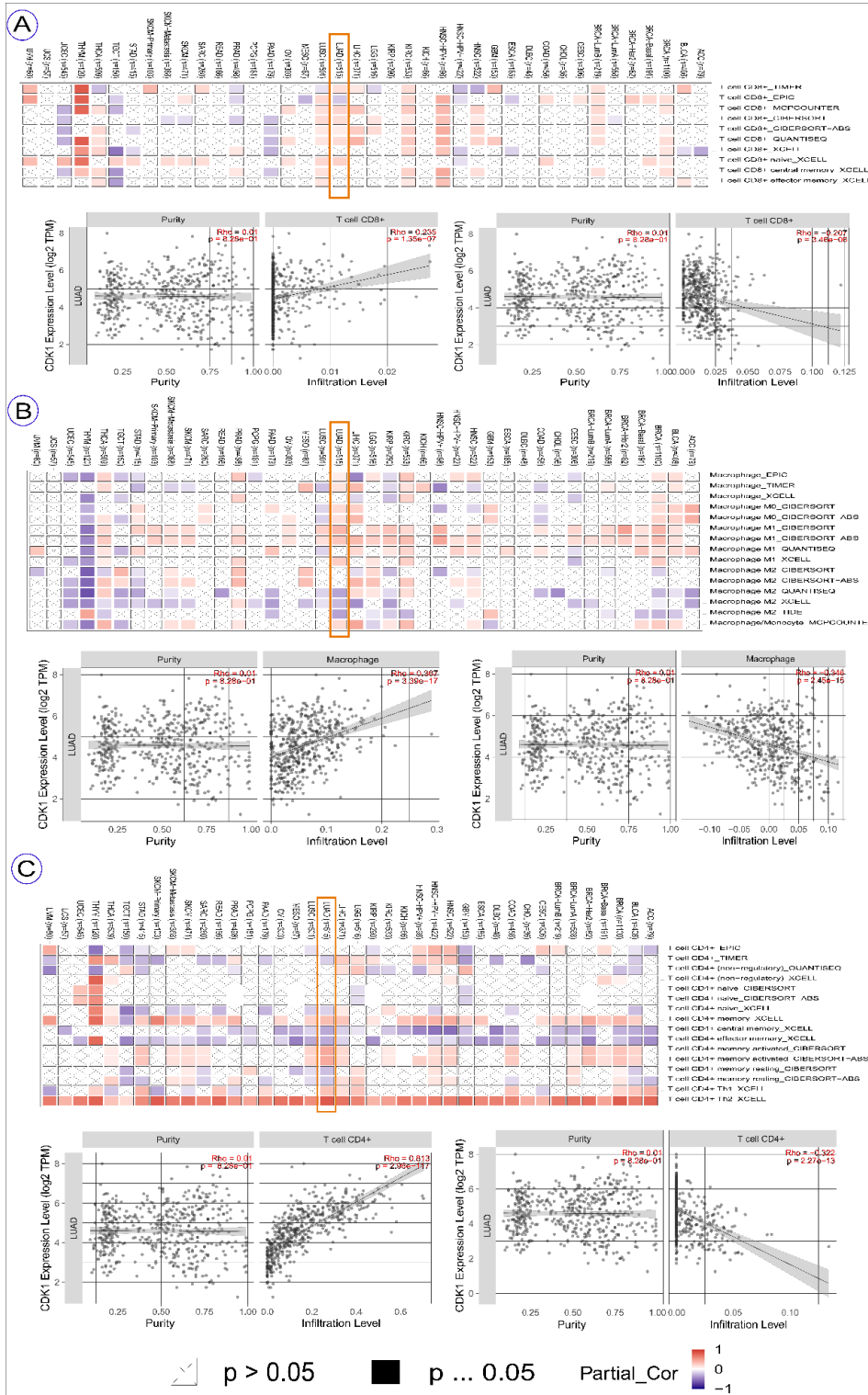


Figure S1. Correlation of CDK1 Expression with Immune Cell Infiltration in LUAD Across CD8+ T Cells (A), Macrophages (B) and CD4+ T Cells (C).

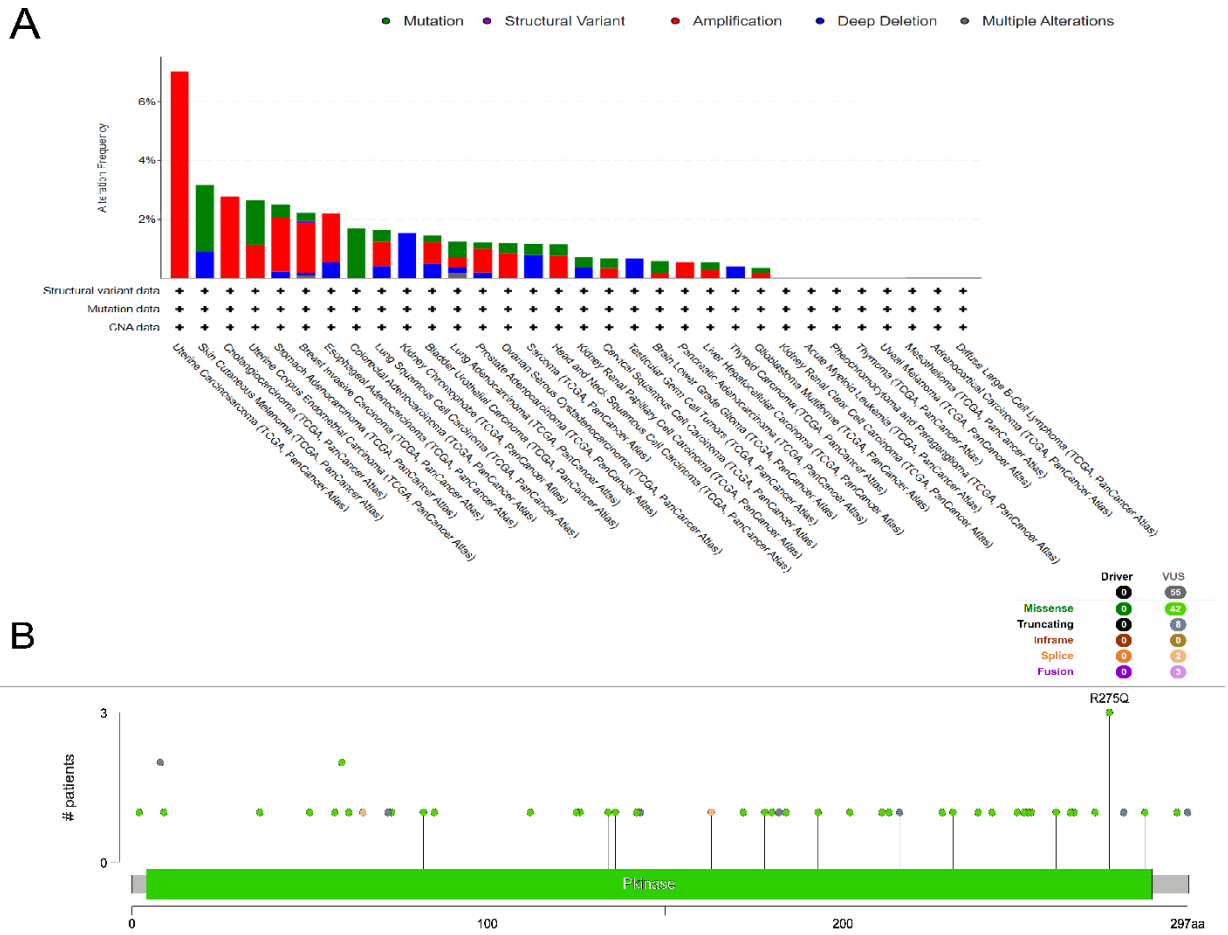


Figure S2. Genetic alterations of CDK1 across cancers. (A) Alteration frequency and types in TCGA datasets. (B) Mutation spectrum and genomic distribution of CDK1 variants.

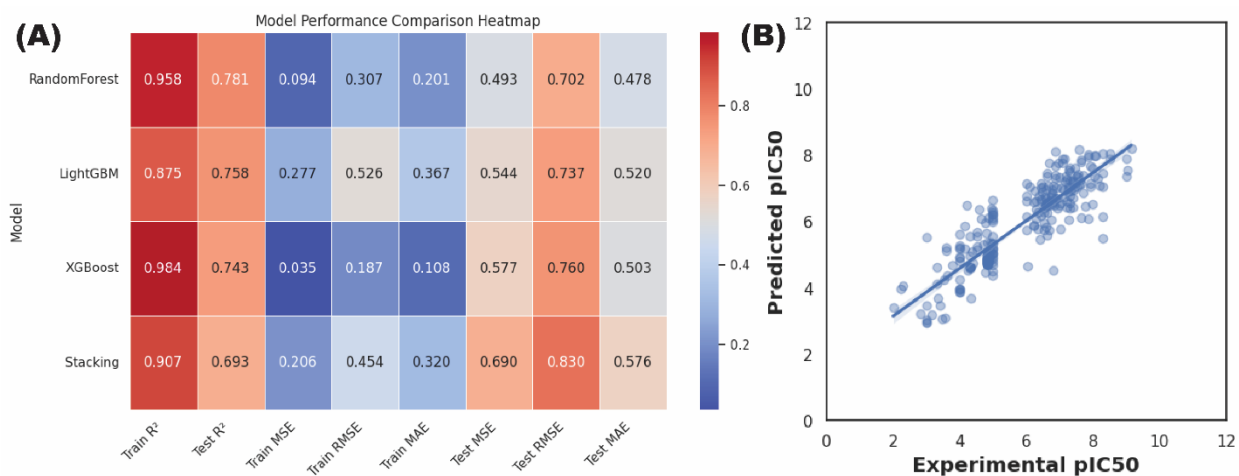


Figure S3. (A) Heatmap illustrating the performance of four machine-learning regression models (RandomForest, XGBoost, LightGBM, and Stacking) across training and testing metrics for CDK1 inhibitor prediction. (B) Scatter plot showing the correlation between experimentally observed pIC50 values and LightGBM-predicted pIC50 values, demonstrating the model's strong predictive accuracy.

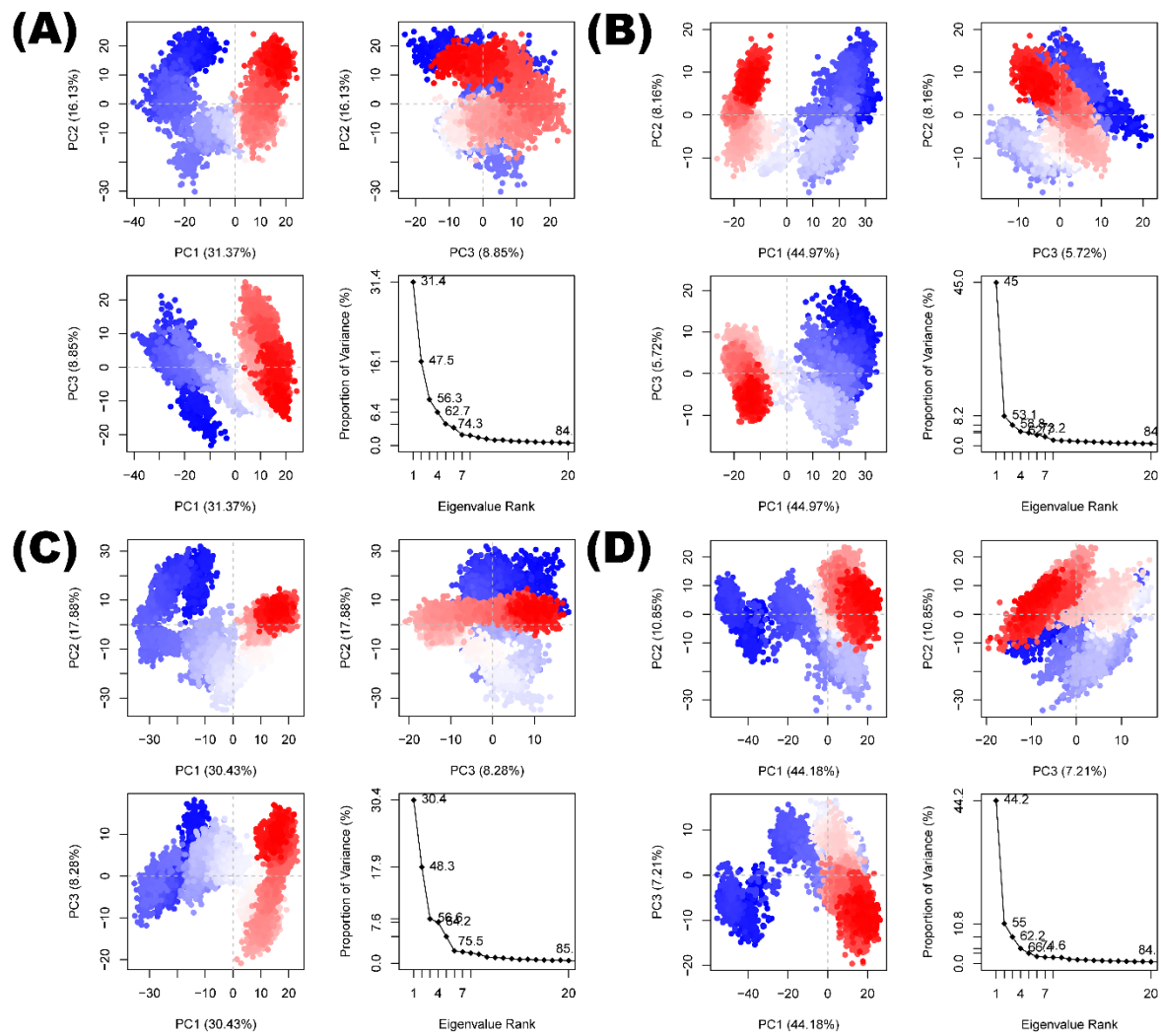


Figure S4. Principal Component Analysis (PCA) Biplots and Scree Plots of CDK1 Complexes: (A) 6GU7_487089, (B) 6GU7_174880, (C) 6GU7_14218027, and (D) Control (AZD5438)

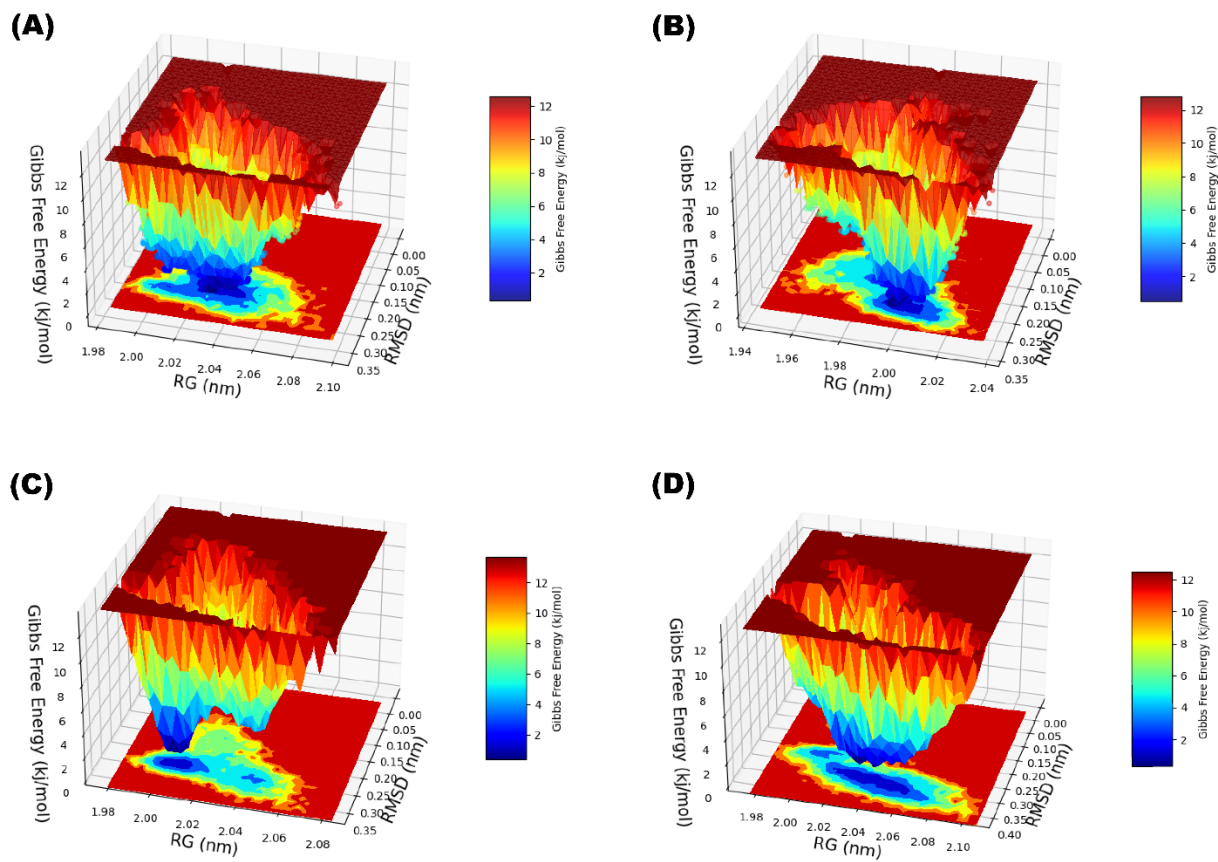


Figure S5. Gibbs Free Energy Landscapes of CDK1-Inhibitor Complexes: (A) 6GU7_487089, (B) 6GU7_174880, (C) 6GU7_14218027, and (D) Control (AZD5438).